Journal of Cellular Biochemistry 96:555–568 (2005)

Co-Localization of PARP-1 and Lamin B in the Nuclear Architecture: A Halo-Fluorescence- and Confocal-Microscopy Study

Melita Vidaković,[2] Mario Koester,[1] Sandra Goetze,[3] Silke Winkelmann,[1] Martin Klar,[1] Goran Poznanović,[2] and Juergen Bode[1]*

[1]GBF, German Research Center for Biotechnology/Epigenetic Regulation, Mascheroder Weg 1, D-38124 Braunschweig, Germany
[2]Molecular Biology Laboratory, Institute for Biological Research, Despot Sephen Blvd. 142, 11060 Belgrade, Serbia and Montenegro
[3]Swammerdam Institute for Life Sciences, University of Amsterdam (UvA), 1098 EL Amsterdam, The Netherlands

Abstract A functional interaction between poly(ADP-ribose) polymerase-1 (PARP-1) and lamin B has recently been proposed by nuclear fractionation, crosslinking, and immunoprecipitation experiments. Here we use fluorescence microscopy to verify and extend these findings. We analyze nuclear halo preparations by fluorescence in situ immuno staining (FISIS), which shares attributes with traditional nuclear fractionation techniques, and by confocal laser scanning microscopy (CLSM). The results agree in that a major part of the enzyme co-localizes with lamin B under physiological conditions, where PARP-1 only has basal activity. After DNA damage and the associated activation of PARP-1, and during the subsequent entry into apoptosis, dramatic changes occur: a gradual release of the enzyme from the lamina, accompanied by its accumulation in nucleoli. Our observations are in line with biochemical evidence for lamin B-PARP-1 interactions under physiological conditions and suggest ways by which these interactions are modified to support PARP-functions in damage and its fate in apoptosis. J. Cell. Biochem. 96: 555–568, 2005.

Key words: PARP-1; interaction partners; nuclear matrix; nuclear lamina; lamin B; functional compartmentalization; nucleolus; halo-FISIS; confocal laser scanning microscopy

Chromatin is a dynamic, hierarchically organized entity, which not only packages DNA but also permits local changes in DNA structure in response to various stimuli. Since its discovery, poly(ADP-ribosyl)ation has been linked to almost every aspect of chromatin structure and DNA metabolism, in particular to the process of DNA repair [Kreimeyer et al., 1984; Rouleau et al., 2004].

The responsible enzyme, poly(ADP-ribose) polymerase-1 (PARP-1; EC 2.4.2.30), a 113 kDa DNA-binding protein of 1,014 amino acid residues [de Murcia and Menissier-de Murcia, 1994; Oei et al., 1997], is constitutively expressed in eukaryotic cells where it comprises up to 1% of total nuclear proteins. Using nicotinamide adenine dinucleotide (NAD^+) as a substrate it modifies certain proteins by ADP-ribose polymers in response to DNA damage

Abbreviations used: BRCT, BRCA1-terminus; CLSM, confocal laser scanning microscopy; Cy3, indocarbocyanine; DAPI, 4′,6-diamidino-2-phenylindole; FISH, fluorescent in situ hybridization; FISIS, fluorescent in situ immuno staining; FITC, fluorescein isothiocyanate; Gy, Gray (energy dose caused by ionzing radiation); kDa, kiloDalton; NAD^+, nicotinamide adenine dinucleotide; PARP-1, poly(ADP-ribose) polymerase-1; PCNA, proliferating cell nuclear antigen; S/MAR, scaffold/matrix attachment region; SSBR, single-strand break repair.

Grant sponsor: DAAD Fellowship (to M.V.); Grant number: A/03/30128; Grant sponsor: Deutsche Forschungsgemeinschaft; Grant number: BO 419-6; Grant sponsor: INTAS (to J.B.); Grant number: 011-0279.

*Correspondence to: Juergen Bode, GBF, German Research Center for Biotechnology/Epigenetic Regulation, Mascheroder Weg 1, D-38124 Braunschweig, Germany.
E-mail: jbo@gbf.de

Received 16 February 2005; Accepted 23 March 2005
DOI 10.1002/jcb.20516

[d'Amours et al., 1999; Tong et al., 2001; Sukhanova et al., 2004]. Although several less abundant PARP-like proteins have been identified [Smith et al., 1998; Kickhoefer et al., 1999], it appears that about 90% of protein-bound ADP-ribose polymers are assembled by PARP-1. Most of these polymer chains are covalently attached to PARP-1 itself [automodification, see Ref. Rolli et al., 2000], and to a limited number of other DNA-binding proteins involved in either chromatin architecture (histones H1, H2B, HMG proteins, lamin B, and nucleolar proteins like B23) [Augustin et al., 2003], or DNA metabolism (replication factors and topoisomerases) [de Murcia and Menissier-de Murcia, 1994; d'Amours et al., 1999; de Murcia and Shall, 2000].

Poly(ADP-ribosyl)ation represents a molecular link between DNA damage and chromatin modification and thereby an obligatory step in the signaling pathway that leads to the repair of strand breaks [Shall and de Murcia, 2000]. In cases genetic damage cannot be repaired, the cell triggers apoptosis, a process that involves the proteolytic cleavage and thereby inactivation of PARP-1 [Kauffman et al., 1993; Lazebnik et al., 1994; d'Amours et al., 1999]. A more recent aspect is the non-covalent association of poly(ADP-ribose) with nuclear proteins, among these the tumor suppressor p53 and lamins, which bind to free and PARP-1 bound chains of the polymer. Both binding modes are mediated by a binding motif shared by many proteins involved in DNA repair [Pleschke et al., 2000] suggesting that poly(ADP-ribose) serves as a scaffold for the assembly of the DNA repair machinery.

In an unchallenged cell the constitutive levels of the ADP-ribosyl chains are low since PARP-1 only has basal activity [Wielckens et al., 1983]. Under these conditions the majority of ADP-ribose residues found on acceptor proteins are mono- or oligo(ADP-ribose) units and thereby different from the higher oligomeric chains that occur at times of damage [Benjamin and Gill, 1980; Alvarez-Gonzalez and Jacobson, 1987]. Since most published studies are devoted to the function of PARP-1 in cells responding to DNA damage, little is yet known about the enzyme's sub-nuclear distribution under physiological conditions. Reports dealing with this aspect [Cardenas-Corona et al., 1987; Alvarez-Gonzalez and Ringer, 1988; Quesada et al., 1994; Vidaković et al., 2004] agree, however, that a major fraction of the enzyme is tightly associated with the nuclear matrix.

The nuclear matrix (otherwise called "nuclear scaffold") has first been isolated as a three-dimensional structure that remains after extraction of soluble nuclear proteins [Gerace and Burke, 1988]. Since then much evidence has accumulated to show that the spherical structure, which consists of a peripheral nuclear lamina, an inner fibrogranular network, and residual nucleoli [Nickerson, 2001], is derived from an entity that provides both skeletal and functional support in a functional cell. Lamins, the major protein constituents, form a mesh that underlies the nuclear membranes. Two major types, lamins A and B, can be distinguished. While the B-type lamins are encoded by distinct genes [Pollard et al., 1990; Biamonti et al., 1992], the A-type lamins (lamin proteins A and C) arise from a single gene by alternative splicing [Lin and Worman, 1993; Furakawa et al., 1994; Machiels et al., 1996]. In addition to their forming the nuclear lamina there is more recent evidence indicating that both A- and B-type lamins may participate in intranuclear [Bridger et al., 1993; Moir et al., 1994; Hozak et al., 1995; Broers et al., 1997] and transnuclear tube-like structures [Fricker et al., 1997].

PARP-1 recurs as a component of nuclear matrix-associated multiprotein complexes [Alvarez-Gonzalez and Ringer, 1988] with implications in DNA repair, replication, and transcription [d'Amours et al., 1999]. A common effect of nuclear protein poly(ADP-ribosyl)ation in these events might be the alteration of chromatin structures [Poirier et al., 1982; Huletsky et al., 1989; Rouleau et al., 2004], which could involve major substrates such as the lamins [Pedraza-Reyes and Alvarez-Gonzalez, 1990] and topoisomerase II [Scovassi et al., 1993]. Since PARP-1 resides in regions of the nuclear matrix that establish contacts with scaffold/nuclear matrix attachment regions (S/MARs), it is in the position to efficiently influence higher-order chromatin structures [Galande and Kohwi-Shigematsu, 1999].

By protein–protein interaction- and co-immunoprecipitation-studies we have previously shown that under physiological conditions, where the enzyme has only basal activity, about 70% of PARP-1 is associated with the nuclear matrix. Within this compartment lamin B is the predominant interaction partner. The

present report examines the subnuclear distribution of PARP-1 by methods that preserve the nuclear architecture, that is, in situ by a recently developed halo-extraction procedure (called either halo-FISH or halo-FISIS, depending on the labeled constituent) or in the "frozen" in vivo state using confocal microscopy. The results confirm that a significant population of PARP-1 co-localizes with lamin B under basal conditions. They also demonstrate that, after PARP-1 is activated by γ-irradiation, the association is altered. Further changes are traced during apoptosis at higher doses of γ-irradiation.

MATERIALS AND METHODS

Cell Culture

Murine Hepa 1-6 is a mouse hepatoma cell line (DSMZ ACC 175) derived from the BW7756 tumor that arose in a C57L mouse; secreting several liver-specific products such as albumin, α1-antitrypsin, α-fetoprotein, amylase. Hepa cells were maintained in Dulbecco's modified Eagle medium (DMEM) supplemented with 10% fetal calf serum, 60 μg/ml penicillin, 100 μg/ml streptomycin, and 5 μM L-glutamine.

γ-Irradiation of Hepa Cells

Hepa cells were plated onto 100 mm^2 cell culture dishes, trypsinized, and washed three times with phosphate-buffered saline pH 7.4 (PBS). Irradiation at doses of 5 and 75 Gy was performed at room temperature in DMEM equilibrated with 5% CO_2, by a 1.5 or 22 min exposure to a ^{137}Cs γ-source. This source contained two 16.5E12 Bq elements corresponding to doses of 204.6 Gy/h [Model OB29/4, STS Steuerungstechnik und Strahlenschutz GmbH, Braunschweig; see Ref. Kronholz et al., 1998]. After each irradiation step, cells were maintained in medium for 15 min at room temperature and afterwards placed on ice. They were subsequently used for scaffold isolation and preparation of nuclear halos. For confocal microscopy, cells grown in 60 mm dishes on glass coverslips were irradiated in dishes/medium without trypsinization and incubated at room temperature as described above.

In Situ Preparation of Nuclear Halos

Control Hepa cells were trypsinized, washed twice with PBS, and incubated on ice with CSK buffer (10 mM Pipes, 100 mM NaCl, 0.3M sucrose, 30 mM $MgCl_2$, and 1% Triton X-100) for 15 min. Irradiated Hepa cells were treated the same like control: two times washing in PBS and 15 min incubation in CSK buffer. Control and irradiated Hepa cell nuclei were counted and 1.5×10^4 nuclei in 50 μl were pelleted onto slides using a cytospin centrifuge (800 rpm for 5 min). The slides were treated with extraction buffer (0.25M $(NH_4)_2SO_4$, 10 mM Pipes (pH 6.8), 10 mM EDTA, 0.1% digitonin, 0.05 mM spermine, and 0.125 mM spermidine) for 3 min to extract histones and soluble proteins. This extraction procedure releases DNA loops from the nuclear remnants resulting in halo structures [Goetze et al., 2003; Heng et al., 2004]. The slides were then subjected to a series of 10×, 5×, 2×, and 1× PBS washes followed by a series of rinses at 70%, 90%, and 100% ethanol concentrations. They were air-dried and fixed at 60–70°C for 2 h. After heating slides were frozen until use.

Fluorescence In Situ Immuno Staining (FISIS)

Immunofluorescence microscopy. Slides prepared as described above were thawed and brought to room temperature, washed twice in PBS supplemented with 0.2% Tween 20 (PBS/Tween) and blocked for 1 h in blocking buffer (Roche Diagnostics, Mannheim, Germany). After one washing step, they were incubated with the first primary anti-PARP-1 antibody (Roche and Santa Cruz, H-250) for 1 h at room temperature, in a dark humidity chamber. The slides were washed three times with PBS/Tween, incubated with the second primary anti-lamin B antibody (M-20 and H-90; Santa Cruz Biotechnology, Santa Cruz, CA) for 1 h at room temperature. Primary antibodies were used at 1:100 dilutions in PBS/Tween. After five washes in PBS/Tween, the slides were incubated with a mixture of fluorescently labeled secondary antibodies, indocarbocyanine (Cy3)-labeled goat anti-(rabbit IgG) secondary antibody, at 1:800 dilutions (Dianova, Hamburg, Germany) for PARP-1 detection, and fluorescein (FITC)-labeled donkey anti-(goat IgG) secondary antibody at a dilution 1:100 (Dianova, Hamburg, Germany) for lamin B detection. Excess antibody was removed by five washes with PBS/Tween. The slides were stained with 4′,6-diamidino-2-phenylindole (DAPI—0.187 μg/ml in Vectashield mounting medium) and analyzed by fluorescence microscopy using appropriate filters. Fluorescence microscopy was performed with a Zeiss

Axiovert 135TV microscope equipped for epifluorescence. Filter sets from OmegaOptical were used for DAPI (XF113), FITC (XF100), and Cy3 (XF111) visualization. Images were acquired with a photometric (Tucson, AZ) high-resolution, cooled charge-coupled device camera (PXL 1400, Grade 2) for 12-bit image collection controlled by IPLab Spectrum software (Signal-Analytics).

Confocal Analysis

Hepa cells grown on glass coverslips were fixed with cold (−20°C) methanol/acetone (1:1) for 10 min at room temperature. The cells were permeabilized with 0.2% Triton X-100 in PBS (pH 7.4) for 10 min, washed three times in PBS and blocked with 3% bovine serum albumin (BSA) in PBS supplemented with 0.2% Tween 20 (PBS/Tween) for 1 h. The slides were incubated 1 h at 4°C with the first primary antibody, anti-PARP-1 (Roche and Santa Cruz, H-250), in a dark humidity chamber. In the next step, the slides were washed five times with PBS/Tween, incubated with the second primary antibody, the anti-lamin B antibody (M-20 and H-90 (data not shown); Santa Cruz Biotechnology) for 1 h at room temperature. After five washes with PBS/Tween, the slides were incubated with the mixture of fluorescent secondary antibodies as above, washed five times with PBS/Tween and mounted on glass slides with Mowiol (Calbiochem). Confocal imaging was performed with a Zeiss LSM 510 META inverted laser-scanning microscope using a Plan-Apochromat 100× oil immersion objective (1.3 numeric apertures). FITC-labeled antigens were excited with an argon laser at 488 nm, and emission was monitored using a 505–550 nm bandpass filter. For Cy3-labeled antibodies a HeNe laser with 543 nm and a 560–615 nm bandpass filter was used. To exclude fluorescence cross-talk under our imaging conditions we determined the cross-emission for both fluorophores. No significant bleeding-through of Cy3 and FITC into the unspecific color channel was detected.

Nuclear Scaffold Preparation Procedure

For the preparation of nuclear scaffolds with intact DNA loops Hepa cells were washed twice with ice-cold isolation buffer (IB: 3.75 mM Tris-HCl pH 7.4, 0.05 mM spermine, 0.125 mM spermidine, 0.5 mM K-EDTA, 1% thiodiglycol, 0.1 mM phenyl methyl sulphonyl fluoride, PMSF), and scraped off the plate with 7.5 ml of IB supplemented with 0.1% digitonin. The cells were homogenized by 14 strokes in a tight-fitting Dounce homogenizer and centrifuged at 900 × g for 5 min at 4°C. After two strokes in a loose-fitting Dounce homogenizer, the homogenized cells were pelleted at 900 × g for 5 min at 4°C. The pellet was resuspended in 200 μl of nuclear buffer (5 mM Tris-HCl, pH 7.4, 0.05 mM spermin, 0.125 mM spermidine, 20 mM KCl, 1% thiodiglycol, 0.2 mM PMSF, and 10 μg/ml aprotinin), and heat stabilized for 30 min at 42°C. After 30 min in nuclear buffer, 4 ml of freshly prepared lithium 3,5-diiodosalicylate (LIS) buffer (25 mM LIS, 20 mM *N*-(2-hydroxyethyl) piperazine-*N*′-2-ethanesulfonic acid (HEPES)-NaOH, pH 7.4, 0.1M lithium acetate, 1 mM EDTA, 0.1% digitonin) was added and the nuclear pellet was carefully homogenized by two strokes in a loosely fitting Dounce homogenizer. After centrifugation (5,000 × g, 5 min, 4°C) the pellet consisting of nuclear scaffolds was transferred to a centrifuge tube containing 20 ml of sterile-filtered restriction buffer (20 mM Tris-HCl, pH 7.4, 0.05 mM spermin, 0.125 mM spermidine, 20 mM KCl, 70 mM NaCl, and 10 mM $MgCl_2$). The tube was gently rocked for 30 min at room temperature and centrifuged as before; this step was repeated at least twice. Nuclear scaffolds were then resuspended in storage buffer (0.25m sucrose, 10 mM $MgCl_2$, 20 mM Tris-HCl (pH 7.4), and 1 mM PMSF) with 5% of glycerol and transferred into 1.5 ml tubes. Before nuclear scaffolds were used for Western blotting, they were digested with 100 U/ml DNase I over night.

Western Immunoblot Analysis

Twenty micrograms of nuclear scaffolds separated by SDS–PAGE were electroblotted onto a nitrocellulose membrane. Western analysis was performed using following antibodies: polyclonal anti-lamin B (M-20; Santa Cruz Biotechnology) (1:2,000 dilution), polyclonal anti-PARP-1 (Roche, Germany) (1:2,000 dilution), monoclonal anti-p53 (Santa Cruz Biotechnology) (1:500 dilution), monoclonal anti-p21 (Santa Cruz Biotechnology) (1:500 dilution), and monoclonal anti-PCNA antibody (Santa Cruz Biotechnology) (1:500 dilution). Western immunoblots were visualized by chemiluminescence (Santa Cruz Biotechnology) according to the manufacturer's specifications.

Poly(ADP-Ribose) Polymerase Assay

PARP activity assays were carried out according to Quesada et al. [2000] with minor modifications. The reaction mixture (final volume 50 μl) contained 100 mM Tris-HCl pH 8, 14 mM β-mercaptoethanol, 10 mM $MgCl_2$, 400 μM (^{14}C)NAD^+ (10,000 cpm/nmole) and isolated nuclear scaffolds corresponding to 100 μg protein as the enzyme source. The nuclear scaffolds were not digested with DNase I to allow examination of PARP-1 activation in response to DNA strand-breaks as a result of irradiation. After 30 min of incubation at 30°C, the reaction was stopped by the addition of ice-cold trichloroacetic acid 40% (v/v) and the radioactivity in the acid-insoluble material was measured in a Beckman LS8100 liquid scintillation counter. One milliunit (mU) is defined as the amount of enzyme activity catalyzing the incorporation per minute of 1 nmole of ADP-ribose into acid-insoluble material.

RESULTS

In Situ Localization of PARP-1 and Lamin B in the Nuclear Matrix: Halo-FISIS

In previous work we have shown that a major portion of PARP-1 co-fractionates with the nuclear matrix and we performed the conventional protein interaction approaches to demonstrate that lamin B is its primary binding partner. We wanted to follow the fate of the enzyme during DNA damage and apoptosis by fluorescence microscopy and to this end we have used an alternative miniscale-preparation approach, the halo extraction procedure [Heng et al., 2004], by which DNA loops and matrix portions can be fixed on a microscopic slide. Preparations of this type are well suited for both FISH (fluorescence in situ hybridization, see Ref. Goetze et al., 2003) and FISIS (fluorescence in situ immunostaining, see Ref. Goetze et al., 2005) analyses by which DNA or matrix-associated proteins can be shown, respectively. During the process nuclei are immobilized on slides before soluble proteins are extracted whereby gross rearrangements of macromolecular contacts are prevented. The FISIS approach applied here requires homogenous and well-defined cells capable of growing on cover slips. As most of our previous findings were performed on liver cells, we used the Hepa 1-6, hepatoma cell line for the present study.

To evaluate the PARP-1-nuclear lamina association status in situ, histone-depleted nuclear halos were prepared by extracting cell nuclei with 0.25M $(NH_4)_2SO_4$ and 1% Triton X-100. Emanating DNA loops were visualized by DAPI, a DNA-specific dye (Fig. 1a), as a halo surrounding the nuclear matrix. The preparations were subsequently stained with an anti-lamin B antibody (Fig. 1b) and with an anti-PARP-1 antibody (Fig. 1c). Binding was monitored by FITC- or by Cy-3-labeled secondary antibodies, respectively. Figure 1 demonstrates thread-like structures for lamin B (b) and PARP-1 (c). In addition, PARP-1 aggregates of varying size are visible, which cannot be assigned to particular nuclear compartments such as nucleoli.

For the thread-like structures a spatial relationship between both components becomes visible: if images are superimposed, a yellow rim of overlap occurs (d), indicating co-localization

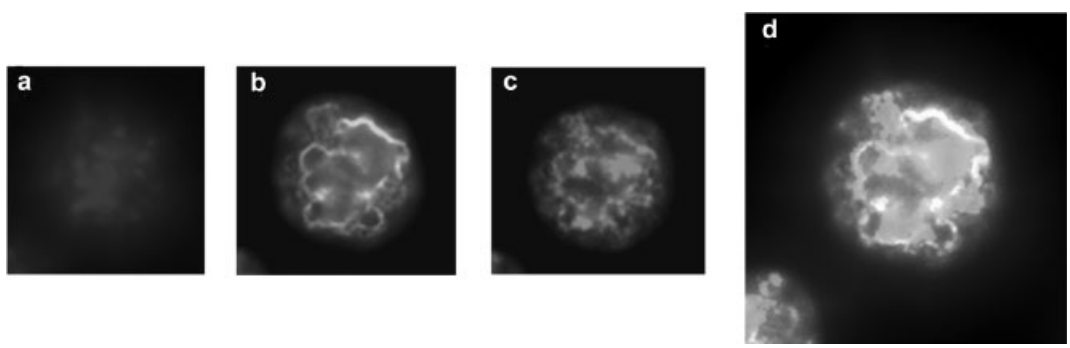

Fig. 1. FISIS analysis of tricolor-stained control nuclear halos. Control nuclear halos were stained with: (**a**) DAPI for visualizing DNA; (**b**) anti-lamin B antibody (M-20, Santa Cruz), visualized with FITC-labeled secondary antibody (green) and (**c**) anti-PARP-1 antibody (Roche) visualized with Cy3-labeled secondary antibody (red). **Panel d**, superimposed image (yellow-overlapping regions). [Color figure can be viewed in the online issue, which is available at www.interscience.wiley.com.]

for a population of PARP-1, and lamin B molecules. These together with previous results [Vidaković et al., 2004] suggest that this overlap indicates a functional interaction between the two components.

PARP-1-Lamin B Co-Localization In Vivo: Confocal Analyses

Nuclear halo preparations represent a situation intermediate between classical isolated nuclear matrix structures and preparations as they are used for confocal analyses of intact cells. Confocal imaging permits the investigation of complete cells after the physiological status has been fixed. This technique has the potential to provide the most stringent evidence for a PARP-1-lamin B co-localization in vivo.

Information on the intranuclear localization of PARP-1-lamin B complexes was derived from optical sections on Hepa cells using a CLS-microscope. Figure 2 shows typical PARP-1 and lamin B patterns for double-stained cells. Anti-lamin B epitopes are stained green (b), and anti-PARP-1 epitopes red (a) in the same nucleus. Panel (b) reflects the typical lamin B distribution: lamin B appears as a smooth green ring reflecting the nuclear contour. For panel (a) PARP-1 staining displays granules throughout the nucleoplasm in addition to a continuous rim at the nuclear periphery, but no staining of the nucleoli.

Co-localization of both proteins is observed at the nuclear periphery and for at least those parts of the interior where both patterns overlap within the precision limits of the procedure (panel c). This interior staining may either reflect the presence of a lamin veil as postulated by Goldman et al. [2002] or it may be due to an invagination of the nuclear membrane. For Figure 2, panel (d) we have superimposed densitometric scans for both channels, red (PARP-1) and green (lamin B) along the path indicated in panel c (white line). These line measurements will be compared with the corresponding data for cells after γ-irradiation (Fig. 5, below). So far the results confirm that lamin B and a significant portion of nuclear PARP-1 are in close proximity at the nuclear envelope in vivo.

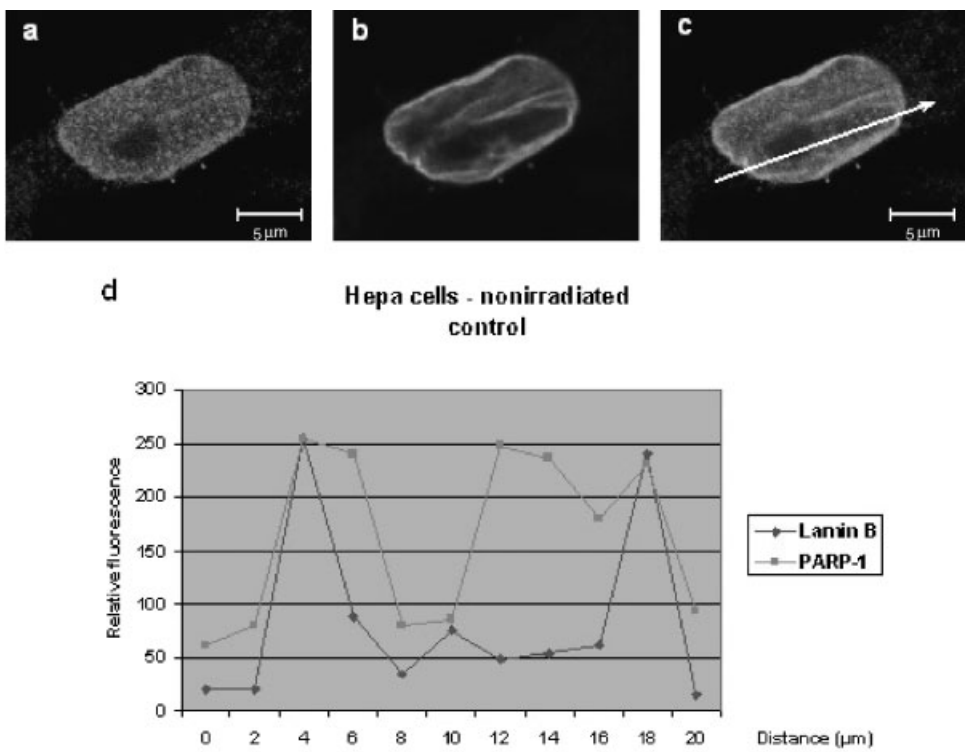

Fig. 2. Confocal analysis of PARP-1 and lamin B by double staining of control Hepa cells. Hepa cells were fixed and subsequently stained with: (**a**) anti-PARP-1 antibody (Roche) (Cy3-red); (**b**) anti-lamin B antibody (M-20, Santa Cruz) (FITC-green); (**c**) superimposed image (regions of overlap are in yellow). Densitometric scans for both channels, red (PARP-1) and green (lamin B) are presented at **panel d**. [Color figure can be viewed in the online issue, which is available at www.interscience.wiley.com.]

Activity Changes of PARP-1 Following γ-Irradiation of Hepa Cells

In living cells, PARP-1 activity is directly proportional to the number of single- and double-strand breaks. It can increase as much as 500-fold [Simonin et al., 1993]. In addition both, constitutive levels and levels of ADP-ribose polymers after PARP-1 activation, depend on the NAD^+ concentration. In order to induce strand breaks in a graded and reproducible manner, Hepa cells were exposed to defined doses of γ-irradiation.

The involvement of PARP-1 in DNA repair was assessed by determining its activity in the isolated scaffolds before and after exposure to increasing doses of γ-irradiation. Subsequent to a 15 min incubation period at room temperature, the 5 Gy dose had increased the activity of PARP-1 36-fold (insert to Fig. 3). The irradiation dose that induced apoptosis was 75 Gy (Fig. 3; lane 3) as judged from the appearance of its 89 kDa proteolytic fragment, which is ascribed to PARP-1 cleavage by caspases 3 and 7 [Tewari et al., 1995; Germain et al., 1999; Slee et al., 2001]. After this treatment PARP-1 activity had decreased as a consequence of degradation but it still exceeded the control 17-fold (Fig. 3, insert).

These results were supplemented by immuno-blot analyses performed on isolated scaffolds in order to correlate the presence and expression patterns of PARP-1 and lamin B with typical DNA repair markers (Fig. 3). To this end the scaffolds were probed with antibodies against to p53, proliferating cell nuclear antigen (PCNA), and p21 [Fritsche et al., 1993; Chin et al., 1997; Frouin et al., 2003]. While the PARP-1 antibody detected the full length 113 kDa form for the control (lane 1) and for scaffolds after irradiation with 5 Gy (lane 2), it revealed a contribution of the 89 kDa apoptotic fragment after irradiation with 75 Gy in addition to the intact molecule (lane 3), as anticipated. When stained for p53, PCNA, and p21, the scaffolds were positive even at the low (5 Gy) dose (lane 2). Under both conditions PARP-1 as well as the lamins became poly(ADP-ribosyl)ated [Vidaković, 2005; data not shown]. However, the late apoptotic phase that occurs between 10 and 15 h post treatment [Horky et al., 2001] and which involves the degradation of lamins as well as other nuclear and nucleolar proteins is not attained in this

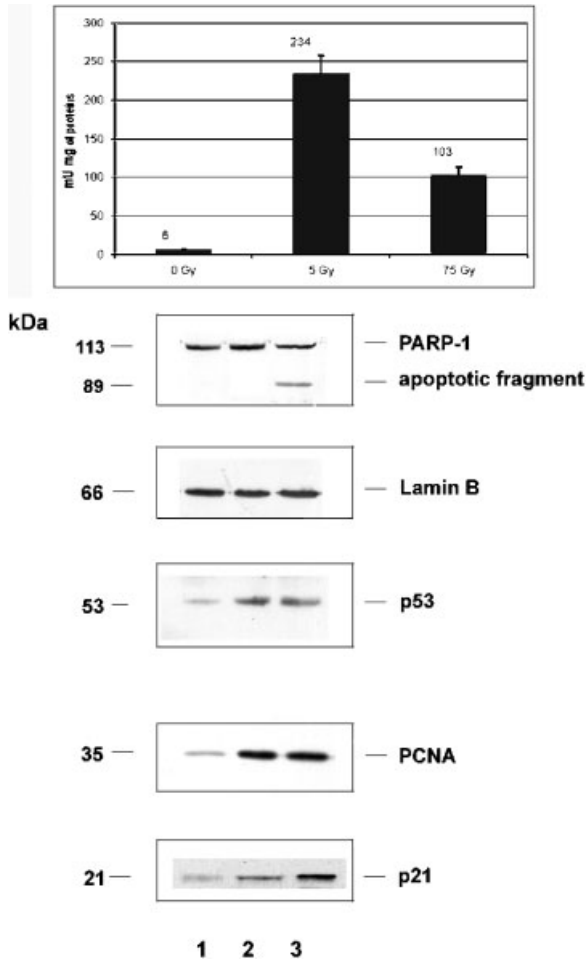

Fig. 3. Western analysis of the isolated nuclear scaffolds after γ-irradiation. **Lane 1**-control scaffolds; **lane 2**-scaffolds after irradiation with 5 Gy; **lane 3**-scaffolds after irradiation with 75 Gy. All samples were probed with: anti-PARP-1, anti-lamin B, anti-PCNA, anti-p53, and anti-p21 antibodies. The values of PARP-1 activity in the inset are averages from at least three different experiments.

study (see the constant signal for lamin B in Fig. 3).

In brief, these results confirm that irradiation of Hepa cells with 5 Gy leads to the induction of DNA repair, accompanied by PARP-1 activation and elevated expression of p53, PCNA, and p21. Irradiation at 75 Gy initiates the apoptotic process. In the following these two dose-dependent states were chosen for co-localization studies in order to examine the distribution patterns of the activated and partially inhibited PARP-1 and lamin B.

FISIS Analyses on Irradiated Nuclear Halos

So far analyses have established co-localization of a significant portion of PARP-1 and lamin

B for the basal state by biochemical [Vidaković et al., 2004] and fluorescence microscopy studies (Figs. 1 and 2). How is this distribution changed by DNA damage and apoptosis? Figure 4 (panel a–d) shows the immunofluorescent staining of nuclear Hepa cell halos 15 min after irradiation with 5 Gy. Depending on the focus, both lamin B and PARP-1 overlapped to a reduced, but still visible extent within the nuclear halo structure. This was confirmed by merging the two images (panel d) where yellow remnants represent some residual co-localization at the nuclear matrix. We conclude that a 5 Gy dose not only triggers PARP-1 activity (and thereby its automodification) but also starts to affect its association with lamin B since co-localization is now restricted to defined parts of the nucleus.

To examine the effects of doses where inhibition of PARP-1 by caspase-mediated degradation is noted, we analyzed its distribution and that of lamin B in nuclear halos irradiated with 75 Gy (Fig. 4; panels e–h). Figure 4 shows the staining pattern of lamin B (panel f, green color), and the distribution of PARP-1 (panel g, stained red). While zones of overlap were still noted in panel (d), they had almost vanished in panel (h).

Confocal Analysis of PARP-1 and Lamin B Co-Localization After Irradiation of Hepa Cells

While the loss of co-localization with lamin B indicates a redistribution of PARP-1 after its activation, the analyses performed so far do not permit conclusions about its fate. Therefore we performed confocal analyses for each of the above irradiation steps. Hepa cells were grown on glass coverslips and irradiated as above. Fifteen minutes after exposure they were fixed and permeabilized. Figure 5 (panel a–c) shows the nuclear distribution of lamin B and PARP-1 after 5 Gy of irradiation. At a focal plane in the center of the cell the immunostaining still shows a marked peripheral localization of lamin B (panel b). According to the anti-PARP-1 antibody (panel a), however, PARP-1 is now found in evenly distributed granules throughout the nucleus. The superimposition of the two images (panel c and evaluation in panel d) reflects the green lamin B signal at the periphery but barely any yellow components that would indicate a co-localization. Under these conditions, however, a significant co-localization is observed with the PCNA as expected for the prototypical single-strand break repair (SSBR) pathway [Vidaković et al., 2005].

After induction of apoptosis at 75 Gy, the lamin B staining pattern is hardly changed (panel f), whereas PARP-1 starts to be concentrated in the nucleolus (panel e). This agrees with an internally localized maximum in the red trace of the line analysis (panel h). The superimposition of the two images (panel g) demonstrates a complete loss of co-localization between PARP-1 and lamin B.

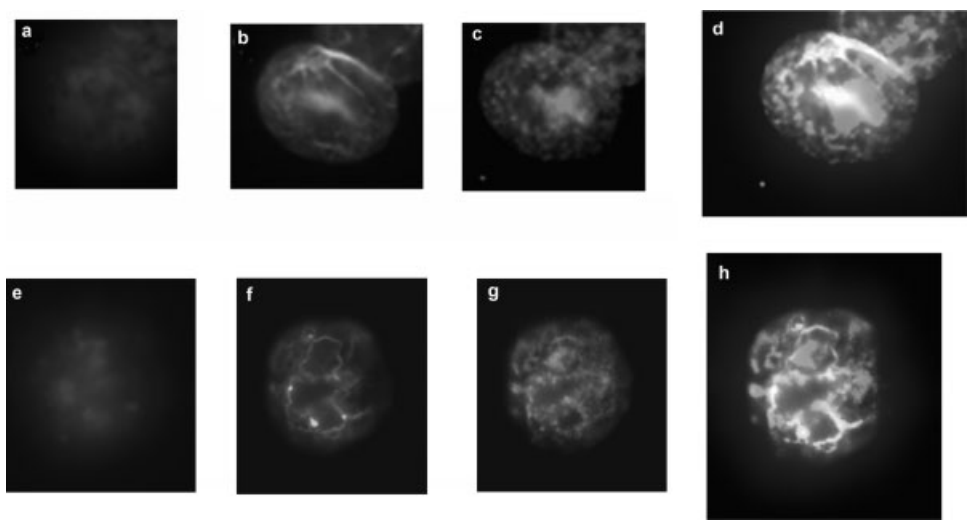

Fig. 4. FISIS analysis of irradiated nuclear halos. Nuclear halos prepared after each irradiation step were tricolor-stained with: (**b**, **f**) anti-lamin B antibody (M-20, Santa Cruz), visualized with FITC-labeled secondary antibody (green) and (**c**, **g**) anti-PARP-1 antibody (Roche) visualized with Cy3-labeled secondary antibody (red). Nuclear halos (**a**, **e**) were stained with DAPI for DNA visualization. **Panels d**, **h** represent the superimposed images. **Panels a–d** display stained halos after irradiation with 5 Gy; **panels e–h** display stained halos after irradiation with 75 Gy. [Color figure can be viewed in the online issue, which is available at www.interscience.wiley.com.]

DISCUSSION

The association of PARP-1 with other proteins is relevant for understanding the enzyme's function in various nuclear compartments. Using a number of conventional fractionation schemes to define the nuclear matrix anchors of PARP-1, we have previously demonstrated that a major portion (up to 80%) of matrix-associated PARP-1 co-fractionates with the lamins. These results have been supported by in vivo crosslinking and co-immunoprecipitation experiments [Vidaković et al., 2004]. In the absence of artifacts, interaction anticipates co-localization in the cellular space. Here we use advanced fluorescence microscopy techniques to verify the co-occurrence of both protein partners. We first investigate the physiological status of the cell where PARP-1 has only basal activity as in our preceding study. Major efforts are then dedicated to trace changes in the co-localization with lamin B that accompany defined stages of DNA damage, DNA-repair, and apoptosis.

Whenever the nuclear localization of PARP-1 has been addressed before, the results did not comply with a universal scheme. This may be ascribed to the variety of cell types investigated, to their physiological status, to the procedure used for inducing DNA damage (and thereby PARP-1 activation) and finally to the methods that have been applied to localize the enzyme. Lankenau et al. [1999] have found that upon PARP-1 activation newly-synthesized poly-(ADP-ribose) polymers occur at the nuclear rim. The automodification of PARP-1 that results from its activation is a salient feature of the poly(ADP-ribosyl)ation process and has therefore served as a convenient marker for its localization. Accordingly, it was assumed that a concentration of poly(ADP-ribose) residues along the nuclear periphery reflects the presence of PARP-1 at the lamina, which itself is subject to modification by PARP-1 [Adolph and Song, 1985]. This observation, however, differs from the enzyme's distribution reported by Desnoyers et al. [1996] for MDBK, HeLa, and CHO cells. Although PARP-1 was found throughout the nuclei according to indirect immunofluorescence, it appeared to be concentrated in the nucleoli. The observation that transcription inhibitors caused its release from these compartments indicated that its nucleolar accumulation depends on ongoing RNA synthesis.

Alvarez-Gonzalez et al. [1999] observed PARP-1 staining throughout the nucleus of HeLa cells without a marked enrichment in the nucleoli. After inducing apoptosis by MNNG-mediated alkylation the nucleolar contribution changed: a translocation of the large apoptotic PARP-1 fragment to the nuclear space was observed 1–2 h after the onset of the treatment. This fragment was poly(ADPribosyl)ated and was proposed to modulate the activity of the apoptotic apparatus. The corresponding small fragment remained in the nucleoli as a possible consequence of its DNA strand break-binding capacity.

In the present study we have compared the subnuclear distribution of PARP-1 and lamin B under various physiological conditions. The basal state of PARP-1 was examined in control cells, its activated form in cells irradiated with 5 Gy, and its partially inhibited state after exposure to 75 Gy during the initial stage of apoptosis (Fig. 3). Our results lead to a model in which an initial co-localization of the interacting partners is gradually lost during successive stages of DNA repair (PARP-1 activation) and apoptosis (PARP-1 inactivation due to caspase action). Early in the apoptotic process a strong PARP-1 signal is generated in the nucleoli, concomitant with the enzyme's inactivation and its subsequent cleavage (Fig. 3). These steps resemble the early apoptotic stages described by Alvarez-Gonzalez et al. [1999].

PARP-1 has long been known to play a role in the recognition of DNA damage caused either directly by genotoxic agents or indirectly by the introduction of DNA-base lesions [Tong et al., 2001]. It has been suggested that, following DNA damage, the enzyme participates in the activation and up-regulation of the tumor suppressor protein p53 [Malanga et al., 1998]. Genes encoding $p21^{WAF1/CIP1}$ and PCNA become in turn subject to regulation by p53 [Paunesku et al., 2001]. By binding to PCNA, p21 can regulate its functions in replication and repair [Waga and Stillman, 1998, review by Vidaković et al., 2005]. There are also recent reports on the role of p53-Mdm2 interactions occurring in the nucleolus prior to p53 export and its degradation at the cytoplasmic proteasomes [Sherr and Weber, 2000]. If these interactions are broken, the half-life of p53 is extended [Rubbi and Milner, 2003]. The growth arrest resulting from these and other contributions provides sufficient time for DNA repair

to be completed before replication starts [Waldman et al., 1995]. For present purposes we chose γ-irradiation to induce DNA strand breaks and to activate PARP-1 in conjunction with p53, PCNA, and p21, which serve as marker proteins for DNA repair (Fig. 3).

Following our previous study, which was centered around the relation of PARP-1 and conventional nuclear matrix preparations [Vidaković et al., 2004], we first applied a novel matrix-visualization technique (here: halo-FISIS) to confirm that, also under physiological conditions, a major proportion of PARP-1 co-localizes with lamin B at the periphery of nuclear halos (Fig. 1). After irradiation the co-localization is gradually lost, indicated by the fact that in Figure 4 red areas (PARP-1) occur in addition to green threads (lamin B) while yellow zones indicating an overlap are largely reduced.

In the halo-FISIS technique the nuclear halo reflects the expanded DNA loops, which, after mild extraction of nuclei, remain attached to the nuclear matrix via S/MARs. The attachment patterns are highly reproducible and their dependence on the presence of S/MARs has been unambiguously demonstrated [Heng et al., 2004]. Careful controls have been applied to overcome objections dealing with the artifactual nature of these preparations [Goetze et al., 2003]. Others have met the same type of criticism by encapsulating cells in agarose microbeads before applying nuclear matrix extraction procedures [Hozak et al., 1995]. While the technique confirms an association of PARP-1 with one of the most prominent nuclear matrix components, it does not permit discrimination between other components of the nuclear matrix such as nucleolar remnants and the internal network. Therefore we have followed these processes in parallel by confocal laser scanning microscopy (CLSM).

Under physiological conditions CLSM reveals a granular, but largely uniform distribution of PARP-1 throughout the nucleoplasm. In addition, there is a population co-localizing with the lamins at the nuclear rim, as detected by a Cy3-fluorescent-labeled antibody. In the case of the standard Hepa cell line PARP-1 was virtually absent from the nucleoli (Fig. 2). HeLa cells showed the same distribution, whereas a marked nucleolar PARP-1 contribution was traced for human osteocarcinoma (MG-63) cells (data not shown). Together with the discrepancies in the literature we have to conclude that differences in PARP-1 distribution depend on the particular cell type and possibly on cell-specific responses to the stress that arises during the respective preparation.

PARP-1 activation by irradiation with a 5 Gy dose clearly results in a more homogeneous but still granular distribution within the nucleus (Fig. 5; panel a). At the same time the co-localization with PCNA becomes a prominent feature [Vidaković, 2005] indicating the onset of the SSBR route: PCNA tethers Pol δ to the complex in a way that is controlled by the cell cycle checkpoint protein p21 with the result that repair is initiated is terminated at the expense of cell cycle progression [review: Vidaković et al., 2005].

At the transition from DNA repair to apoptosis (75 Gy) PARP-1 is translocated from the nucleoplasm to the nucleoli (Fig. 5; panel e) while the population at the nuclear rim is decreased. Considering that the nucleolus is the earliest site of caspase-mediated proteolysis [Stegh et al., 1998; Horky et al., 2001] and that PARP-1 cleavage is one of the earliest apoptotic markers, it is tempting to speculate that these events are inter-related. The interaction between PARP-1 and PCNA that occurs at 5 Gy, becomes limited by PARP-1 degradation after 75 Gy, which in turn is accompanied by its accumulation in the nucleolus [Vidaković et al., 2005]. Nucleolin may be part of this circuitry since an inhibitor of PARP-1 blocks its redistribution during apoptosis. It has been suggested that nucleolin clears dying cells from PARP-1 in a process that may be triggered by its poly(ADP-ribosyl)ation or by its binding to the large 89 kDa PARP-1 fragment [Mi et al., 2003].

What is the possible functional implication of the tight correlation between PARP-1 and lamin B/the lamins in non-apoptotic cells? In higher eukaryotic genomes late replicating chromatin domains are dynamically associated

Fig. 5. Confocal analysis of PARP-1 and lamin B co-localization after irradiation of Hepa cells. Cells were double-stained with: (**a**, **e**) anti-PARP-1 (Roche), displayed in red, and (**b**, **f**) anti-lamin B (M-20, Santa Cruz), displayed in green. **Panels c**, **g** represents superimposed images. Cell stained after irradiation with 5 Gy are represented on **panels a**–c and after 75 Gy of irradiation on **panels d**–**f**. Densitometric scans for both channels, red (PARP-1) and green (lamin B) are presented at panel d for superimposed image after 5 Gy of irradiation and in **panel h** for superimposed image after 75 Gy of irradiation. [Color figure can be viewed in the online issue, which is available at www.interscience.wiley.com.]

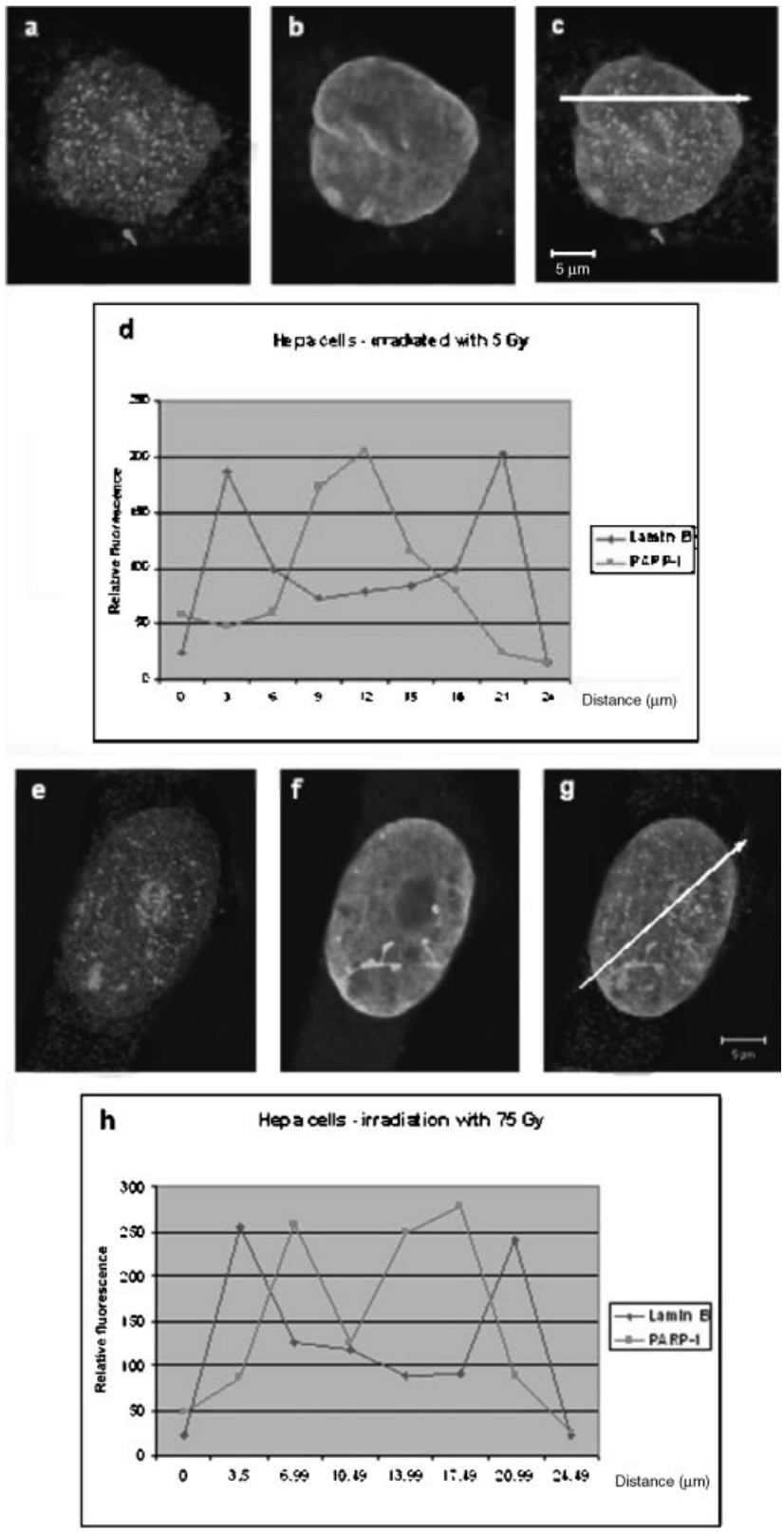
a
b
c
5 µm
d
Hepa cells - irradiated with 5 Gy
Relative fluorescence
Distance (µm)
Lamin B
PARP-1
e
f
g
h
Hepa cells - irradiation with 75 Gy
Relative fluorescence
0
3.5
6.99
10.49
13.99
17.49
20.99
24.49
Distance (µm)
Lamin B
PARP-1

Fig. 5.

with the nuclear envelope as parts of a network of specific protein–protein and protein-DNA interactions [Ehrenhofer-Murray, 2004]. The large diversity of interactions between lamin-binding proteins with DNA and a variety of chromosomal proteins indicate important roles in chromatin organization [review: Foisner, 2002]. A- and B-type lamins have been shown to bind to scaffold/matrix attachment regions in two activity-dependent modes [Ludérus et al., 1994]. PARP-1 shares with the lamins a high affinity for S/MARs and both preferentially recognize DNA secondary structures rather than sequence. Together with the fact that both components are major constituents of the nuclear matrix a synergistic action is an intriguing possibility.

In one scenario poly(ADP-ribosyl)ation of major substrates like histone H1, core histones, and HMG proteins initiates chromatin opening at specific loci. Modification of the lamins would in turn stabilize the open chromatin and release PARP-1 as a consequence of auto- and hetero-modification reactions. As a prerequisite for repair, this process would permit the association of PARP-1 with other S/MARs, which are close by in the nuclear matrix network. Fine tuning could be achieved by different degrees of poly(ADP-ribosyl)ation: while a moderate modification of PARP-1 and lamins could be the prerequisite for a function during DNA repair, a more extensive one could serve their detachment from DNA and their subsequent degradation by caspases.

Further work will have to address the precise mechanism by which PARP-1 and the lamins interact. Two options have been discussed before [Vidaković et al., 2004]. According to the first the interaction is driven by the formation of a coiled-coil involving α-helical regions and/or by the interaction of BRCT modules that are common motifs in DNA repair proteins [Masson et al., 1998]. While this model may be valid for the basal state of PARP-1, the alternative, a poly-(ADP-ribosyl)ation-driven interaction, would require PARP-1 activation. Present work demonstrates that this alternative cannot be effective for high degrees of modification as these release PARP-1 from the lamina.

ACKNOWLEDGMENTS

Melita Vidaković highly appreciates great help of the hosting SAR laboratory at GBF, particularly of Karin Maaß. We thank P.D. Dr. Peter Müller (GBF Braunschweig) for critically reading the manuscript and for fruitful discussions.

REFERENCES

Adolph KW, Song MKH. 1985. Decrease in ADP-ribosylation of HeLa non-histone proteins from interphase to metaphase. Biochemistry 24:345–352.

Alvarez-Gonzalez R, Jacobson MK. 1987. Characterization of polymers of adenosine diphosphate ribose generated *in vitro* and *in vivo*. Biochemistry 26:3218–3224.

Alvarez-Gonzalez R, Ringer P. 1988. Nuclear matrix associated poly(ADP-ribose) metabolism in regenerating rat liver. FEBS Lett 236:362–366.

Alvarez-Gonzalez R, Spring H, Mueller M, Buerkle A. 1999. Selective loss of poly(ADP-ribose) and the 85 kDa-fragment of poly(ADP-ribose) polymerase in nucleoli during alkylation-induced apoptosis of HeLa cells. J Biol Chem 274:32122–32126.

Augustin A, Spenlehauer C, Dumond H, Ménissier-de Murcia J, Piel M, Schmit A, Apiou F, Vonesch J, Kock M, Bornens M, de Murcia G. 2003. PARP-3 localizes preferentially to the daughter centriole and interferes with the G1/S cell cycle progression. J Cell Sci 116:1551–1562.

Benjamin RC, Gill DM. 1980. Poly(ADP-ribose) synthesis *in vitro* programmed by damaged DNA. A comparison of DNA molecules containing different types of strand breaks. J Biol Chem 255:10502–10508.

Biamonti G, Giacca M, Perini G, Contreas G, Zentilin L, Weighardt F, Guerra M, Della Valle G, Saccone S, Riva S. 1992. The gene for a novel human lamin maps at a highly transcribed locus of chromosome 19, which replicates at the onset of S-phase. Mol Cell Biol 12:3499–3506.

Bridger JM, Kill IR, O'Farrel M, Hutchison CJ. 1993. Internal lamin structures within G1 nuclei of dermal fibroblasts. J Cell Sci 104:297–306.

Broers JLV, Machiels BM, Kuijpers HJH, Smedts F, van den Kieboom R, Raymond Y, Ramaekers FCS. 1997. A- and B type lamins are differentially expressed in normal human tissues. Histochem Cell Biol 107:505–517.

Cardenas-Corona ME, Jacobson EL, Jacobson MK. 1987. Endogenous polymers of ADP-ribose are associated with the nuclear matrix. J Biol Chem 262:14863–14866.

Chin PL, Momand J, Pfeifer GP. 1997. *In vivo* evidence for binding of p53 to consensus binding sites in the p21 and GADD45 genes in response to ionizing radiation. Oncogene 15:87–99.

d'Amours D, Desnoyers S, d'Silva I, Poirier G. 1999. Poly(ADP-ribosyl)ation reactions in the regulation of nuclear functions. Biochem J 342:249–268.

de Murcia G, Menissier-de Murcia J. 1994. Poly(ADP-ribose) polymerase: A molecular nick-sensor. Trends Biochem Sci 19:172–176.

de Murcia G, Shall S. 2000. From DNA damage and stress signalling to cell death: Poly(ADP-ribosylation) reactions. New York, Oxford: Oxford University Press, Inc.

Desnoyers S, Kaufmann SH, Piorier GG. 1996. Alteration and the nucleolar localization of poly(ADP-ribose) polymerase upon treatment with transcription inhibitors. Exp Cell Res 227:146153.

Ehrenhofer-Murray AE. 2004. Chromatin dynamics at DNA replication, transcription and repair. Eur J Biochem 271:2335–2349.

Foisner R. 2002. Dynamic connections of nuclear envelope proteins to chromatin and the nuclear matrix. In: Collas P, editor. Nuclear envelope dynamics in embryos and somatic cells. Georgetown: Landes BioSciences.

Fricker M, Hollinshead M, White N, Vaux D. 1997. Interphase nuclei of many mammalian cell types contain deep, dynamic, tubular membrane bound invaginations of the nuclear envelope. J Cell Biol 136:531–544.

Fritsche M, Haessler C, Brandner G. 1993. Induction of nuclear accumulation of the tumor-suppressor protein p53 by DNA damaging agents. Oncogen 8:307–318.

Frouin I, Maga G, Denegri M, Riva F, Savio M, Spadari S, Prosperi E, Scovassi AI. 2003. Human proliferating cell nuclear antigen, poly(ADP-ribose) polymerase-1, and $p21^{waf1/cip1}$ a dynamic exchange of partners. J Biol Chem 278:39265–39268.

Furakawa K, Inagaka H, Hotta Y. 1994. Identification and cloning of an mRNA coding for a germ cell-specific A-type lamin in mice. Exp Cell Res 212:426–430.

Galande S, Kohwi-Shigematsu T. 1999. Poly(ADPR)polymerase and Ku autoantigen form a complex and synergistically bind to matrix attachment sequences. J Biol Chem 274:20521–20528.

Gerace L, Burke B. 1988. Functional organization of the nuclear envelope. Annu Rev Cell Biol 4:335–374.

Germain M, Affar EB, D'Amours D, Dixit VM, Salvesen GS, Poirier GG. 1999. Cleavage of automodified poly(ADP-ribose) polymerase during apoptosis. Evidence for involvement of caspase-7. J Biol Chem 274:28379–28384.

Goetze S, Huesemann Y, Baer A, Bode J. 2003. Functional characterization of transgene integration patterns by Halo-FISH: Electroporation versus retroviral infection. Biochemistry 42:7035–7043.

Goetze S, Baer A, Winkelmann S, Nehlsen K, Seibler J, Maass K, Bode J. 2005. Genomic bordering elements: Their performance at pre defined genomic loci. Mol Cell Biol 25:2260–2272.

Goldman RD, Gruenbaum Y, Moir RD, Shumaker DK, Spann TP. 2002. Nuclear lamins: Building blocks of nuclear architecture. Genes Dev 16:533–547.

Heng HHQ, Goetze S, Ye CJ, Lu W, Liu G, Bremer S, Hughes M, Bode J, Krawetz SA. 2004. Dynamic features of scaffold/matrix attached regions (S/MARs) in anchoring chromatin loops. J Cell Sci 117:999–1008.

Horky M, Wurzer G, Kotala V, Anton M, Vojtesek B, Vacha J, Wesierska-Gadek J. 2001. Segregation of nucleolar components coincides with caspase-3 activation in cisplatin-treated HeLa cells. J Cell Sci 114:663–670.

Hozak P, Sasseville AM, Raymond Y, Cook PR. 1995. Lamin proteins form an internal nucleoskeleton as well as a peripheral lamina in human cells. J Cell Sci 108: 635–644.

Huletsky A, de Murcia G, Muller S, Hengartner M, Ménard L, Lamarre D, Poirier GG. 1989. The effect of poly(ADP-ribosyl)ation on native abd H1-depleted chromatin. A role of poly(ADP-ribosyl)ation on core nucleosome structure. J Biol Chem 264:8878–8886.

Kauffman SH, Desnoyers S, Ottaviano Y, Davidson NE, Poirier GG. 1993. Specific proteolytic cleavage of poly (ADP-ribose) polymerase: An early marker of chemotherapy-induced apoptosis. Cancer Res 53:3976–3985.

Kickhoefer VA, Siva AC, Kedersha NL, Inman EM, Ruland C, Streuli M, Rome LH. 1999. The 193-kD vault protein, VPARP, is a novel poly(ADP-ribose) polymerase. J Cell Biol 146:917–928.

Kreimeyer A, Wielckens K, Adamietz P, Hilz H. 1984. DNA repair-associated ADP-ribosylation *in vivo*. Modification of histone H1 differes from that of the principal acceptor proteins. J Biol Chem 259:890–896.

Kronholz HL, Moustakis C, Wuellenweber S. 1998. Anlage zur bestrahlung von blutkomponenten—technik, dosimetrie und voschläge zur qualitätssicherung. Infusionsther. Transfusionsmed 25:56–61.

Lankenau S, Bürkle A, Lankenau DH. 1999. Detection of poly(ADP-ribose) synthesis in Drosophila testes upon gamma-irradiation. Chromosoma 108:44–51.

Lazebnik YA, Kauffmann SH, Desnoyers S, Poirier GG, Earnshaw WC. 1994. Cleavage of poly(ADP-ribose) polymerase by a proteinase with properties like ICE. Nature 371:346–347.

Lin F, Worman HJ. 1993. Structural organization of the human gene encoding nuclear lamin A and nuclear lamin C. J Biol Chem 268:16321–16326.

Ludérus MEE, Den Blaauwen JL, De Smit OJB, Compton DA, Van Driel R. 1994. Binding of matrix attachment regions to lamin polymers involves single-stranded regions and the minor groove. Mol Cell Biol 14:6297–6305.

Machiels BM, Zorenc AHG, Endert JM, Kuijpers HJH, van Eys GJJM, Ramaekers FCS, Broers JLV. 1996. An alternative splicing product of the lamin A/C gene lacks exon 10. J Biol Chem 271:9249–9253.

Malanga M, Pleschke JM, Kleczkowska HE, Althaus FR. 1998. Poly(ADP-ribose) Binds to specific domains of p53 and alters its DNA binding functions. J Biol Chem 273: 11839–11843.

Masson M, Niedergang C. Schreiber V, Muller S. de Murcia JM, de Murcia G. 1998. XRCC1 Is specifically associated with poly(ADP-Ribose)polymerase and negatively regulates its activity following DNA damage. Mol Cell Biol 18: 3563–3571.

Mi Y, Thomas SD, Xu X, Casson LK, Miller DM, Bates PJ. 2003. Apoptosis in leukemia cells is accompanied by alterations in the levels and localization of nucleolin. J Biol Chem 278:8572–8579.

Moir RD, Montag-Lowy M, Goldman RD. 1994. Dynamic properties of nuclear lamins: Lamin B is associated with sites of DNA replication. J Cell Biol 125:1201–1212.

Nickerson AJ. 2001. Experimental observations of a nuclear matrix. J Cell Sci 114:463–474.

Oei SL, Griesenbeck J, Schweiger M. 1997. The role of Poly(ADP-ribosyl)ation. Rev Physiol Biochem Pharmacol 131:4135–4137.

Paunesku T, Mittal S, Protic M, Oryhon J, Korolev SV, Joachimiak A, Woloschak GE. 2001. Proliferating cell nuclear antigen (PCNA): Ringmaster of the genome. Int J Radiat Biol 77:1007–1021.

Pedraza-Reyes M, Alvarez-Gonzalez R. 1990. Oligo(3′-deoxy ADP-ribosyl)ationof the nuclear matrix lamins from rat liverutilizing 3′-deoxy NAD as a substrate. FEBS Lett 277:88–92.

Pleschke JM, Kleczkowska HE, Strohm M, Althaus FR. 2000. Poly(ADP-ribose) binds to specific domains in DNA

damage checkpoint proteins. Biol Chem 275:52, 40974–40980.

Poirier GG, de Murcia G, Jongstra-Bilen J, Niedergang C, Mandel P. 1982. Poly(ADP-ribosyl)ation of polynucleosomes causes relaxation of chromatin structure. Proc Natl Acad Sci USA 79:3423–3427.

Pollard KM, Chan EKL, Grant BJ, Sullivan KF, Tan EM, Glass CA. 1990. In vitro posttranslational modification of lamin B cloned from a human T-cell line. Mol Cell Biol 10:2164–2175.

Quesada P, d'Erme M, Parise G, Faraone-Minnella MR, Caifa P, Farina B. 1994. Nuclear matrix associated poly(ADP-ribosyl)ation system in rat testis chromatin. Exp Cell Res 214:351–357.

Quesada P, Tramontano F, Faraone-Minnella MR, Farina B. 2000. The analysis of the poly(ADPR) polymerase mode of action in rat testis nuclear fractions defines a specific poly(ADP-ribosyl)ation system associated with the nuclear matrix. Mol Cell Biochem 205:91–99.

Rolli V, Ruf A, Augustin A, Schulz GE, Menissier de Murcia J, de Murcia G. 2000. Poly(ADP-ribose)polymerase structure and function and poly ADP-ribosylation reactions. In: de Murcia G, Shall S, editors. From DNA damage and stress signaling to cell death. New york, Oxford: Oxford University Press, Inc. p 35.

Rouleau M, Aubin RA, Poirier GG. 2004. Poly(ADP-ribosyl)ated chromatin domains: Access granted. J Cell Sci 117:815–825.

Rubbi CP, Milner J. 2003. Disruption of the nucleolus mediates stabilization of p53 in response to DNA damage and other stress. EMBO J 22:6068–6077.

Scovassi AI, Mariani C, Negroni M, Negri C, Bertazzoni U. 1993. ADP-ribosylation of nonhistorne proteins in HeLa cells: Modification of DNA topoisomerase II. Exp Cell Res 206:177–181.

Shall S, de Murcia G. 2000. Poly(ADP-ribose) polymerase-1: What have we learned from the deficient mouse model? Mutat Res 460:1–15.

Sherr JC, Weber JD. 2000. The ARF/p53 pathway. Curr Opin Genet Develop 10:94–99.

Simonin F, Poch O, Delarue M, de Murcia G. 1993. Identification of potential active-site residues in the human poly(ADP-ribose) polymerase. J Biol Chem 268:8529–8535.

Slee EA, Adrain C, Martin SJ. 2001. Executioner caspase-3, -6 and -7 perform distinct, non-redundant roles during the demolition phase of apoptosis. J Biol Chem 276: 7320–7326.

Smith S, Giriat I, Schmitt A, de Lange T. 1998. Tankyrase, a poly(ADP-ribose) polymerase at human telomeres. Science 282:1484–1487.

Stegh AH, Schickling O, Ehret A, Scaffidi C, Peterhansel C, Hofmann TG, Grummt I, Krammer PH, Peter ME. 1998. DEDD, a novel death effector domain-containing protein, targeted to the nucleolus. EMBO J 17:5974–5986.

Sukhanova MV, Lavrik OI, Khodyreva SN. 2004. Poly (ADP-ribose) polymerase-1: A regulator of protein–nucleic acid interactions in processes responding to genotoxic impact. Mol Biol 38:706–717.

Tewari M, Quan LT, O'Rourke K, Desnoyers S, Zeng Z, Beidler DR, Poirier GG, Salvesen GS, Dixit VM. 1995. Yama/CPP32 beta, a mammalian homolog of CED-3, is a CrmA-inhibitable protease that cleaves the death substrate poly(ADP-ribose) polymerase. Cell 81:801–809.

Tong WM, Cortes U, Wang ZQ. 2001. Poly(ADP-ribose) polymerase: A guardian angel protecting the genome and suppressing tumorigenesis. Biochim Biophys Acta 1552: 27–37.

Vidaković M. 2005. Association of poly(ADP-ribosyl) polymerase-1 (PARP-1; EC 2.4.2.30) with the nuclear matrix. Academic Dissertation, University of Belgrade/Faculty of Biology.

Vidaković M, Grdović N, Quesada P, Poznanović G, Bode J. 2004. Poly(ADP-ribose) polymerase-1 association with the peripheral nuclear lamina in rat hepatocytes. J Cell Biochem 93:1155–1168.

Vidaković M, Poznanović G, Bode J. 2005. DNA break repair: Refined rules of an already complicated game. Biochem Cell Biol (in press).

Waga S, Stillman B. 1998. Cyclin-dependent kinase inhibitor p21 modulates the DNA primer recognition complex. Mol Cell Biol 18:4177–4187.

Waldman T, Kinzler KW, Vogelstein B. 1995. p21 is necessary for the p53-mediated G1 arrest in human cancer cells. Cancer Res 55:5187–5190.

Wielckens K, George E, Pless T, Hilz H. 1983. Stimulation of poly(ADP-ribosyl)ation during Ehrlich Ascites tumor cell "starvation" and suppression of concomitant DNA fragmentation by benzamide. J Biol Chem 258:4098–4104.